ChemComm

COMMUNICATION

View Article Online
View Journal | View Issue



Cite this: *Chem. Commun.*, 2023, **59**, 4970

Received 7th March 2023,
Accepted 28th March 2023

DOI: 10.1039/d3cc01135f

rsc.li/chemcomm

# Selective enhancement of organic dye properties through encapsulation in rotaxane orientational isomers†

Leonardo Andreoni, ‡[ab] Federica Cester Bonati, ‡[c] Jessica Groppi,[b] Davide Balestri,[c] Gianpiero Cera,[c] Alberto Credi,[ab] Andrea Secchi *[c] and Serena Silvi *[bd]

**We report the synthesis and characterisation of [2]rotaxanes based on a stilbazolium dye and a calix[6]arene macrocycle. Since both components are non-symmetric, two orientational isomers are obtained. The two isomers display distinct photophysical and photochemical properties in solution and solid state, superior to the unencapsulated dye.**

Stilbazolium salts are push–pull dyes comprising a pyridinium electron acceptor and an electron donor unit bridged by a double bond. They are studied as fluorescent sensors[1–3] and non-linear optical materials;[4–7] moreover, depending on their substituents, they can undergo *E*–*Z* photoisomerisation around the central double bond.[8,9] On account of the charge-transfer character of their electronic transitions,[10] the photophysical properties of these cationic dyes strongly depend on their environment, and they can be affected by encapsulation within the cavity of hosts in supramolecular complexes.[11–13] In this regard, recently, some of us have studied the association of a stilbazolium axle within the cavity of a calix[6]arene macrocycle.[14] Since the host and the guest are non-symmetric, the resulting pseudorotaxane complex displays two possible orientational isomers. In solution, these isomers are both present and exhibit different emission spectra. The ratio between the two isomers can be adjusted by modifying the temperature, but their continuous interconversion prevents their separation. In this study, we investigate rotaxanes **1-Up** and **1-Down**, wherein the stilbazolium-based axle **2** is encapsulated in the calix[6]arene **3** wheel, which directs its upper or lower rim towards the 3,5-dimethyl piperidine unit of the axle, respectively (Fig. 1). Thanks to the mechanical bond, the separation of the isomers is achieved, allowing a thorough investigation of the system in solution and in the solid state. Although different examples of rotaxane orientational isomers are reported in the literature,[15–20] usually they exhibit similar photophysical properties.[15,20] On the other hand, the encapsulation inside the

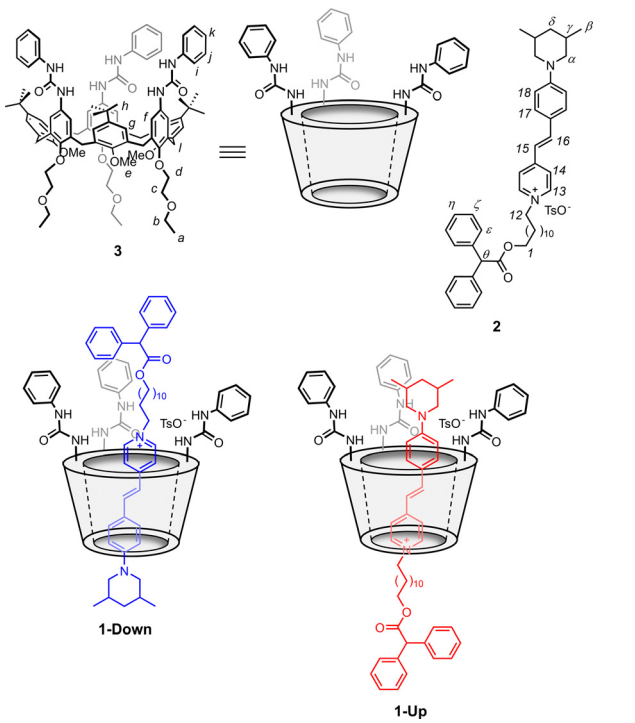


Fig. 1 Chemical structure of axle **2** and the [2]rotaxane orientational isomers **1-Down** and **1-Up** (letters and numbers on the structure of **2** and **3** are used for NMR assignment).

[a] *Dipartimento di Chimica Industriale "Toso Montanari", Università di Bologna, viale del Risorgimento 4, 40136 Bologna, Italy*
[b] *Center for Light-Activated Nanostructures (CLAN), Università di Bologna and Consiglio Nazionale delle Ricerche, via Gobetti 101, 40129 Bologna, Italy*
[c] *Dipartimento di Scienze Chimiche, della Vita e della Sostenibilità Ambientale, Università di Parma, Parco Area delle Scienze 17/A, 43124 Parma, Italy*
[d] *Dipartimento di Chimica "G. Ciamician", Università di Bologna, via Selmi 2, 40126 Bologna, Italy*

† Electronic supplementary information (ESI) available: Compounds synthesis, NMR and optical characterisation, X-ray crystal structure of **1-Down**. CCDC 2243944. For ESI and crystallographic data in CIF or other electronic format see DOI: https://doi.org/10.1039/d3cc01135f

‡ These authors contributed equally.

calix[6]arene cavity improves either the fluorescence or the photoisomerisation of the stilbazolium, depending on the relative orientation of the axle and the wheel. Therefore, the same stilbazolium unit in the two orientational isomers displays different and complementary properties, in both cases superior with respect to the original dye.

To evaluate the effect of axle orientation on the spectroscopic properties of stilbazolium-based rotaxanes, we designed a non-symmetric axle (**2**) endowed with 3,5-dimethyl piperidine and a diphenylacetyl stopper, which prevent axle slippage from the calix[6]arene cavity different accesses.

The monostoppered precursor of **2**, the stilbaziolium tosylate salt **4**, was synthesised in good overall yield (see ESI†). Its complexation by calix[6]arene **3** in low polarity solvents led to the formation of a mixture of two orientational pseudorotaxane isomers **P-Up** and **P-Down** (Scheme 1), as witnessed by the ratio of the $^1$H NMR signals of the piperidine methyl groups ($\beta$) (see Fig. S25, ESI†).§ The axle ω-hydroxymethyl group was then capped with diphenylacetyl chloride, thus locking the orientation of the axle with respect to the non-symmetric calix[6]arene wheel. The resulting oriented rotaxanes **1-Up** and **1-Down** could be isolated by TLC separation in 31 and 37% of yields (45 : 55 ratio) as bright orange and yellow solids, respectively.

The orientation of the axle with respect to the cavity rims was inferred through 1D and 2D NMR measurements (see also ESI†). The $^1$H NMR spectra of the orientational rotaxane isomers **1-Up** and **1-Down** (Fig. 2c and d) are compared with that of its pristine pseudorotaxane mixture (Fig. 2b) and the free axle **2** (Fig. 2a). The axle encapsulation is evidenced by the upfield shift experienced by the axle resonances upon threading (*cf.* Fig. 2a and b–d). The proposed orientation of **2** in the isolated rotaxanes **1-Up** and **1-Down** was supported by monitoring the chemical shift variation of the piperidine unit α methylene protons. In **1-Up**, such protons (3.32 and 1.89 ppm) are slightly upfield-shifted than in **1-Down** (3.64 and 2.11 ppm) because of their engulfment in the aromatic cavity of **3**. These findings were further confirmed thanks to a selective 1D ROE experiment on rotaxane **1-Up**, which showed the proximity of the protons α′ of the dumbbell dimethylpiperidine stopper with the aromatic protons of the wheel phenylureas (see Fig. S14, ESI†).

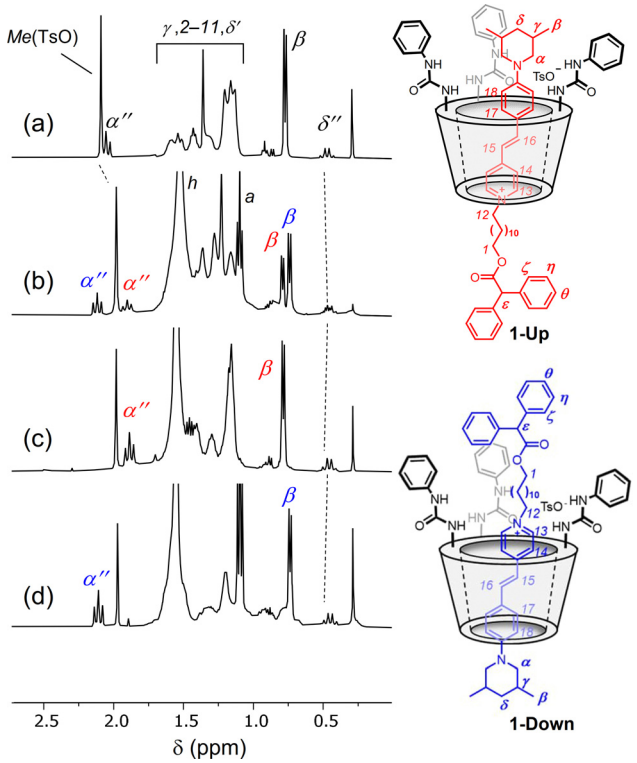


Fig. 2 High fields expansion of $^1$H NMR stack plot showing (a) axle **2**, (b) 1 : 1 mixture of orientational pseudorotaxane isomers **P-Up** and **P-Down**, (c) rotaxane **1-Up**, and (d) rotaxane **1-Down**. All the spectra were taken at 400 MHz in $C_6D_6$ except **2**, recorded in $CD_3OD$ for solubility reasons. For the full stack plot, see Fig. S25, ESI.†

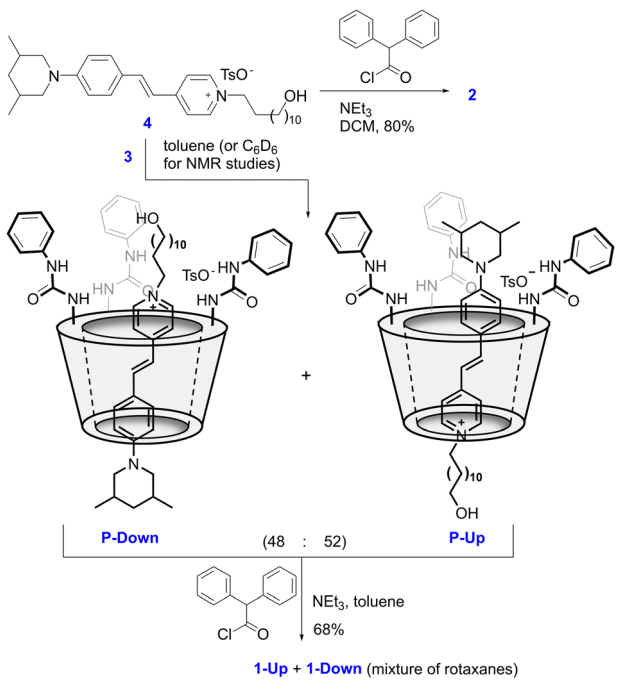


Scheme 1 Synthesis of stilbazolium axle **2** (top) and the mixture of orientational [2]rotaxane isomers **1-Up** and **1-Down** (bottom).

The photophysical and photochemical characterisation was performed in toluene, the results are gathered in Table 1. The absorption and emission spectra of compound **2** depend on its concentration, as they are affected by the ion pairing equilibrium between the stilbazolium ion and its tosylate counterion (see Fig. S26–S28, ESI†). Upon addition of an excess of tosylate counterion, the ion-paired **2** shows an absorption band centred at 450 nm and an emission band at 618 nm ($\Phi_f$ = 18%). In the spectral window of the selected solvent, the absorption spectra of the rotaxanes show only the band related to the stilbazolium unit (Fig. 3), which is independent of the concentration (see Fig. S29, ESI†) but affected by the calix[6]arene and by its orientation with respect to the stilbazolium unit (Fig. 3 and Table 1). Indeed, in analogy with parent pseudorotaxanes,[14] **1-Up** and **1-Down** show distinct absorption bands centred at 468 nm and 425 nm, respectively. Even more pronounced effects of the calix[6]arene orientation are observed in the emission spectra of the rotaxanes:

Table 1 Photophysical and photochemical data of the investigated compounds

| | Toluene | | | | | | Solid | | |
|---|---|---|---|---|---|---|---|---|---|
| Compound | $\lambda_{abs}$/nm | $\lambda_{em}$/nm | $\Phi_{fluo}$ (%) | $\Phi_{EZ}$ (436 nm) (%) | $\Phi_{ZE}$ (436 nm) (%) | $k_{Z\rightarrow E}$[b]/s$^{-1}$ | $\lambda_{abs}$/nm | $\lambda_{em}$/nm | $\Phi_{fluo}$ (%) |
| **2**[a] | 450 | 618 | 18 | 14 | 42 | $3 \times 10^{-4}$ | 451 | 613 | 1 |
| **1-Up** | 468 | 561 | 83 | 7 | 71 | $1 \times 10^{-4}$[c] | 463 | 587 | 11 |
| **1-Down** | 425 | 533 | 20 | 36 | 41 | $\sim 10^{-7}$ | 440 | 576 | 32 |

[a] Properties determined in the presence of an excess of tosylate counterion (see ESI). [b] Rate constant of the thermal $Z \rightarrow E$ isomerisation at room temperature. [c] A minor secondary process is observed; see ESI for details.

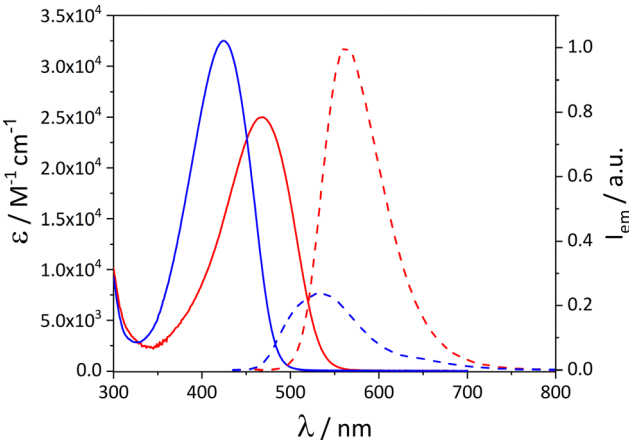


Fig. 3 Absorption (full lines) and emission spectra (dashed lines) of toluene solutions of **1-Up** (red lines, $\lambda_{ex}$ = 454 nm) and **1-Down** (blue lines, $\lambda_{ex}$ = 425 nm). The emission spectra intensity is proportional to the fluorescence quantum yield (0.83 for **1-Up** and 0.20 for **1-Down**).

the two isomers show distinct spectra (Fig. 3 and Tables 1), and **1-Up** is characterised by a fluorescence quantum yield of 83%, *i.e.*, four times larger than **1-Down** and ion-paired **2**.

A rationalisation of these effects is not straightforward, nevertheless, a qualitative explanation of the observed phenomena is attempted. As for the absorption properties, stilbazolium ions exhibit negative solvatochromism,[10] *i.e.* a blue-shifted absorption on increasing the polarity of the media, which would suggest that in **1-Down** the calixarene host provides a more polar environment to the guest than in **1-Up**.

With regard to the emission properties, the smaller Stokes shift and larger quantum yield of **1-Up** can possibly be accounted for by a deeper encapsulation of the stilbazolium and/or a more rigid environment. Indeed, the ground and excited states exhibit different polarities,[10] therefore the energy of the emission can be influenced by the solvent reorganisation. A deeper encapsulation would minimise this effect, as the cavity of the macrocycle may screen the solvent. Moreover, stilbazolium fluorescence can benefit from the presence of an environment that limits molecular rotations.[11]

The influence of encapsulation on the properties of the stilbazolium unit was also investigated in the solid state. Indeed, the inclusion of stilbazolium fluorophores in a restricted environment, such as a macrocyclic cavity[6,7] or a molecular organic framework (MOF),[4,5] is known to prevent the intermolecular π–π stacking responsible for the aggregation caused quenching (ACQ)[21] and enhance the emission in the solid state. The absorption and the emission spectra of the solid compounds resemble the ones observed in solution (see Fig. S35 and S36, ESI†) and, in particular, the two orientational isomers show distinct spectra (Table 1). The emission of **2** is weak ($\Phi_f$ = 1%) due to ACQ, while **1-Up** and **1-Down** exhibit a stronger fluorescence ($\Phi_f$ = 11% and 32%, respectively), as a consequence of the encapsulation of the stilbazolium unit inside the calix[6]arene cavity. To the best of our knowledge, this is the first example of such an enhancement obtained through a rotaxane architecture.

The larger quantum yield of **1-Down** with respect to **1-Up** (an opposite outcome with respect to what was observed in solution) is possibly related to the conformation assumed by the rotaxane in the solid state. To further investigate this aspect, we attempted the crystallisation of the rotaxanes. We successfully isolated crystals suitable for X-ray diffraction analysis from the diffusion of hexane into a toluene solution of **1-Down**. The solved X-ray structure confirms the identity of this orientational isomer (Fig. 4 and Fig. S53–S56, ESI†).§ Considerable effort has been devoted to growing crystals of the **1-Up** isomer, but the size and quality necessary for X-ray diffraction experiments could not be achieved, thus preventing further considerations.

The photoisomerisation processes of axle **2** and rotaxanes **1** were investigated through UV-Vis and NMR spectroscopy (see ESI†). Upon irradiation of the ion-paired **2** at 436 nm, a modest decrease of the absorption band, ascribed to the *E* to *Z* photoisomerisation reaction, is observed (see Fig. S43, ESI†). Upon keeping the solution

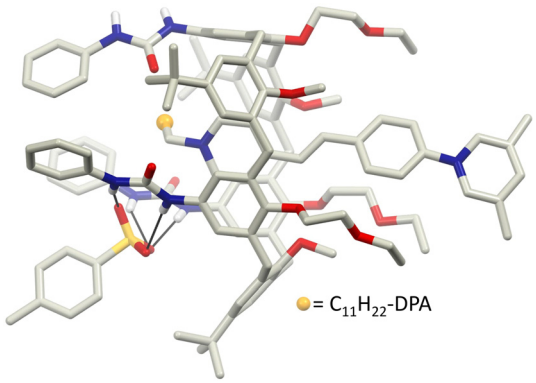


Fig. 4 X-Ray molecular structure of **1-Down** showing the hydrogen bond interactions between the phenylureas N–H groups and the tosylate anion. The disordered alkyl chain bearing the diphenylacetic stopper is depicted as a gold sphere, while hydrogen atoms, except those involved in hydrogen bonding, have been omitted for clarity (see ESI† for further details).

 

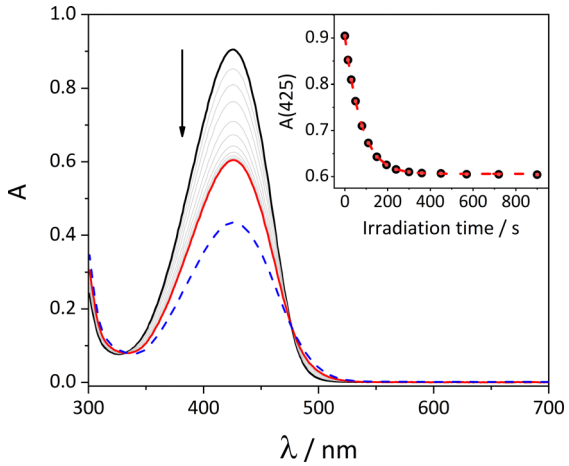


Fig. 5 Absorption spectra of a toluene solution of *E* **1-Down** ($2.8 \times 10^{-5}$ M, black to red lines) upon irradiation at 436 nm. The calculated spectrum of *Z* **1-Down** is reported for comparison (blue dashed line). Inset: Absorption changes at 425 nm (black dots) together with the fitting of the data (red dashed line).

in the dark, the thermal back isomerisation occurs, leading to the recovery of the initial spectrum within a few hours, with a first-order kinetic constant $k_{Z\rightarrow E} = 3 \times 10^{-4}$ s$^{-1}$ (see Fig. S46, ESI†). The photoisomerisation quantum yields were obtained by fitting the photokinetic profile (Table 1). Also the photochemistry of the stilbazolium moiety is influenced by encapsulation within the calixarene cavity, with a dependence on the orientation of the macrocycle. Indeed, the *E* to *Z* photoisomerisation quantum yield $\Phi_{EZ}$ of **1-Up** is 7%, and its photostationary state (PSS) at 436 nm contains only 10% of *Z* isomer (Table 1). On the other hand, **1-Down** is characterised by a $\Phi_{EZ}$ of 36% and a PSS at 436 nm that contains 64% of the *Z* isomer (Fig. 5 and Table 1). Moreover, the thermal back isomerisation of **1-Down** is much slower with respect to the free axle in solution and to the other rotaxane isomer, and its value could only be estimated ($k_{Z\rightarrow E} \sim 10^{-7}$ s$^{-1}$, see Fig. S47, ESI†). The photoisomerisation quantum yields are in accordance and complementary with the emission quantum yields. The results obtained by NMR spectroscopy are consistent with the UV/Vis studies (Fig. S49–S52, ESI†). It is worth to highlight the signals appearing between 0 and −1 ppm in the $^1$H NMR spectrum of **1-Down** upon photoisomerization: such signals could be assigned to the protons of the alkyl chain shielded by the cavity of the wheel; this might suggest that the isomerization of the stilbazolium unit causes a partial displacement of the macrocycle, forcing the wheel to move toward the opposite end of the axle.

Overall, the encapsulated compound shows an improvement of either the photophysical or photochemical properties with respect to the free axle in solution, with a remarkable and distinctive dependence on the orientation of the macrocycle. Indeed, the "up" orientation favours the radiative decay of the stilbazolium dye, with an emission quantum yield as high as 83%, whereas the "down" orientation fosters the photoisomerisation reaction, leading to the kinetically inert *Z* isomer. This peculiar feature allows to select one property (emission or photoisomerisation) over the other, tailoring the system depending on the desired application.

Remarkably, in this system, the orientation plays a role in the outcome of the properties that is as important as the encapsulation itself. Moreover, the orientational isomers display different emission spectra both in solution and solid state, and this feature gives access to a straightforward way to identify the orientation of the macrocycle. This information is trivial in the present rotaxanes, but it can be crucial when studying more complex mechanically interlocked molecules, in which the application of other techniques (such as X-ray crystallography and NMR spectroscopy) could be limited or their interpretation ambiguous. Indeed, understanding the orientation of the macrocycle can be pivotal to get insights on its movements between different stations, a fundamental aspect in the study of artificial molecular machines.

This work was supported by the Italian MIUR (PRIN 20173L7W8K and PRIN 201732PY3X), and it was carried out within the COMP-HUB Initiative, funded by the "Departments of Excellence" program of the Italian Ministry of Education, University and Research (MIUR, 2018-2020).

## Conflicts of interest

There are no conflicts to declare.

## Notes and references

§ Upon mixing **3** and **4** in $C_6D_6$ at room temperature, the orientational pseudorotaxane isomer **P-Up** is formed preferentially (**P-Up**: **P-Down** = 82: 18). The mixture reaches its equilibrium (48:52) in *ca.* 2 h (see ESI†).

1 P. Fromherz and O. Schenk, *Biochim. Biophys. Acta, Biomembr.*, 1994, **1191**, 299–308.
2 J. N. Wilson, A. S. Brown, W. M. Babinchak, C. D. Ridge and J. D. Walls, *Org. Biomol. Chem.*, 2012, **10**, 8710–8719.
3 H. J. Zo, J. N. Wilson and J. S. Park, *Dyes Pigm.*, 2014, **101**, 38–42.
4 J. Yu, Y. Cui, H. Xu, Y. Yang, Z. Wang, B. Chen and G. Qian, *Nat. Commun.*, 2013, **4**, 2719.
5 Y. Wei, H. Dong, C. Wei, W. Zhang, Y. Yan and Y. S. Zhao, *Adv. Mater.*, 2016, **28**, 7424–7429.
6 H. Dong, Y. Wei, W. Zhang, C. Wei, C. Zhang, J. Yao and Y. S. Zhao, *J. Am. Chem. Soc.*, 2016, **138**, 1118–1121.
7 B. Hua, C. Zhang, W. Zhou, L. Shao, Z. Wang, L. Wang, H. Zhu and F. Huang, *J. Am. Chem. Soc.*, 2020, **142**, 16557–16561.
8 U. Steiner, M. H. Abdel-Kader, P. Fischer and H. E. A. Kramer, *J. Am. Chem. Soc.*, 1978, **100**, 3190–3197.
9 H. Görner and H. Gruen, *J. Photochem.*, 1985, **28**, 329–350.
10 B. Carlotti, G. Consiglio, F. Elisei, C. G. Fortuna, U. Mazzucato and A. Spalletti, *J. Phys. Chem. A*, 2014, **118**, 3580–3592.
11 Z. Li, S. Sun, F. Liu, Y. Pang, J. Fan, F. Song and X. Peng, *Dyes Pigm.*, 2012, **93**, 1401–1407.
12 M. Bojtár, Z. Szakács, D. Hessz, M. Kubinyi and I. Bitter, *RSC Adv.*, 2015, **5**, 26504–26508.
13 A. Paudics, D. Hessz, M. Bojtár, B. Gyarmati, A. Szilágyi, M. Kállay, I. Bitter and M. Kubinyi, *Molecules*, 2020, **25**, 5111.
14 M. Bazzoni, F. Terenziani, A. Secchi, G. Cera, I. Jabin, G. de Leener, M. Luhmer and A. Arduini, *Chem. – Eur. J.*, 2020, **26**, 3022–3025.
15 J. E. H. Buston, J. R. Young and H. L. Anderson, *Chem. Commun.*, 2000, 905–906.
16 A. Arduini, F. Ciesa, M. Fragassi, A. Pochini and A. Secchi, *Angew. Chem., Int. Ed.*, 2005, **44**, 278–281.
17 A. G. Cheetham, T. D. W. Claridge and H. L. Anderson, *Org. Biomol. Chem.*, 2007, **5**, 457–462.
18 C. Talotta, C. Gaeta and P. Neri, *Org. Lett.*, 2012, **14**, 3104–3107.
19 H.-X. Wang, Z. Meng, J.-F. Xiang, Y.-X. Xia, Y. Sun, S.-Z. Hu, H. Chen, J. Yao and C.-F. Chen, *Chem. Sci.*, 2016, **7**, 469–474.
20 M. Bazzoni, L. Andreoni, S. Silvi, A. Credi, G. Cera, A. Secchi and A. Arduini, *Chem. Sci.*, 2021, **12**, 6419–6428.
21 M. K. Bera, P. Pal and S. Malik, *J. Mater. Chem. C*, 2020, **8**, 788–802.